Fungal Genetics and Biology 144 (2020) 103446

Contents lists available at ScienceDirect

Fungal Genetics and Biology

journal homepage: www.elsevier.com/locate/yfgbi

Characterization of a heme-protein responsive to hypoxia in *Paracoccidioides brasiliensis*

Lucas Nojosa Oliveira[a,1], Relber Aguiar Gonçales[b,c], Marielle Garcia Silva[a], Raisa Melo Lima[a], Mariana Vieira Tomazett[a], Juliana Santana de Curcio[a], Juliano Domiraci Paccez[a], Vanessa Rafaela Milhomem Cruz-Leite[a], Fernando Rodrigues[b,c], Patrícia de Sousa Lima[a], Maristela Pereira[a], Célia Maria de Almeida Soares[a,*]

[a] Laboratório de Biologia Molecular, Instituto de Ciências Biológicas, ICB II, Campus II, Universidade Federal de Goiás, Goiânia, Goiás, Brazil
[b] Life and Health Sciences Research Institute (ICVS), School of Medicine, University of Minho, Braga, Portugal
[c] ICVS/3B's – PT Government Associate Laboratory, Braga/Guimarães, Portugal

ARTICLE INFO

Keywords:
Oxygen
Iron deprivation
Fungoglobin
Paracoccidioidomycosis
Murine lung infection

ABSTRACT

Oxygen is fundamental to the life of aerobic organisms and is not always available to *Paracoccidioides* cells. During the life cycle stages, reduced oxygen levels directly affect general metabolic processes and oxygen adaptation mechanisms may play a fundamental role on fungal ability to survive under such condition. Heme proteins can bind to oxygen and participate in important biological processes. Several fungi, including *Paracoccidioides*, express a heme-binding globin (fungoglobin - FglA) presumable to regulate fungal adaptation to hypoxia. However, the characterization of fungoglobin in *Paracoccidioides* spp. has not yet been performed. In this study, we predicted the structure of fungoglobin and determined its level of expression during hypoxic-mimetic conditions. Genomic screening revealed that the fungoglobin gene is conserved in all species of the *Paracoccidioides* genus. Molecular modeling showed biochemical and biophysical characteristics that support the hypothesis that FglA binds to the heme group and oxygen as well. The fungoglobin transcript and proteins are expressed at higher levels at the early treatment time, remaining elevated while oxygen is limited. A *P. brasiliensis fglA* knockdown strain depicted reduced growth in hypoxia indicating that this protein can be essential for growth at low oxygen. Biochemical analysis confirmed the binding of fungoglobin to heme. Initial analyzes were carried out to establish the relationship between FlglA and iron metabolism. The FglA transcript was up regulated in pulmonary infection, suggesting its potential role in the disease establishment. We believe that this study can contribute to the understanding of fungal biology and open new perspectives for scientific investigations.

1. Introduction

Fungi of the *Paracoccidioides* genus are responsible for a life-threatening infection in humans, causing a systemic mycosis known as paracoccidioidomycosis (PCM). The disease is restricted to Latin America and Brazil has the highest number of cases (Martinez, 2017; Restrepo et al., 2001). The lung is the gateway to infection and when conidia or mycelial propagules are inhaled, they differentiate into yeast cells establishing the disease (Brummer et al., 1993). Depending on the predisposition of the host, the fungal infection may be limited to the lung or progress to a systemic mycosis (Bagagli et al., 2008; Brummer et al., 1993), with an estimated occurrence of 3360 to 5600 new cases per year (Martinez, 2017). PCM is the first leading cause of death caused by systemic mycosis in Brazil (Prado et al., 2009).

Despite being considered an obligate aerobe, fungi of the genus *Paracoccidioides* experience oxygen-limiting conditions in their ecological niche and in host tissues (Bagagli et al., 2008; Fortes et al., 2010). Oxygen is an elemental molecule that participates in metabolic processes of aerobic respiration, and is required for the biosynthesis of sterols, heme group, fatty acids and ascorbic acid in aerobic microorganisms (Rocha, 2007). Oxygen concentration is reduced in decomposing organic material layers, as well as in the mammalian lungs, the site of PCM infection (Grahl et al., 2011; Hanslin et al., 2005). The O_2 concentration ranges from 11% to > 1% under conditions of systemic

* Corresponding author at: Laboratório de Biologia Molecular, Instituto de Ciências Biológicas II, Campus Samambaia, Universidade Federal de Goiás, 74690-900 Goiânia, Goiás, Brazil.
E-mail address: celia@ufg.br (C.M. de Almeida Soares).
[1] Present address: Departamento de Biomedicina, Faculdade Estácio de Sá de Goiás, Goiânia, Goiás, Brazil.

https://doi.org/10.1016/j.fgb.2020.103446
Received 20 December 2019; Received in revised form 2 August 2020; Accepted 12 August 2020
Available online 19 August 2020
1087-1845/

normoxia, while lower oxygen levels that have been described in tumors and wounds characterize hypoxic (Arnold et al., 1987; Carreau et al., 2011; Dewhirst, 1998; Simmen et al., 1994).

Metabolic and respiratory adaptations are required for *Paracoccidioides* cells to survive in those environments, and key proteins play an important role in this response. Thus, oxygen-sensing mechanisms induce metabolic responses that enable fungi to adapt to low levels of O_2. Studies of the occurrence of hypoxia in fungal infections have shown severe changes in metabolism, morphology, transcriptional activities, and virulence of the fungal cells (Blatzer et al., 2011; Chang et al., 2007; Hoot et al., 2008; Lima et al., 2015; Synnott et al., 2010; Todd et al., 2006; Vik and Rine, 2001; Willger et al., 2008; Dubois and Smulian, 2016). It has been demonstrated that *Paracoccidioides lutzii* undergoes metabolic changes due to oxygen limitation. At first, proteins from glycolysis, TCA and mitochondrial electron transport chain decreased. However, after 24 h, glycolysis and mitochondrial electron transport chain are reestablished, and gluconeogenesis, the GABA shunt, and beta-oxidation pathways increased. In contrast, proteins from the TCA cycle remain poorly expressed (Lima et al., 2015).

In most human pathogenic fungi, hypoxia sensitization occurs through Sterol Responsive Element Binding Proteins - SREBPs (Blatzer et al., 2011; Chang et al., 2007; Lima et al., 2015; Todd et al., 2006; Willger et al., 2008; Dubois and Smulian, 2016) or the UPC2 transcription factor (Hoot et al., 2008; Synnott et al., 2010; Vik and Rine, 2001), both involved in the expression of hypoxic genes that are related to lipid, ergosterol and heme biosynthesis, ethanol production and iron metabolism. The *P. lutzii* SREBP, known as *Pl*SrbA, was characterized as responsive to hypoxic stress in a previous study (Lima et al., 2015).

Heme-binding proteins may be important in oxygen metabolism because of the high-affinity binding of oxygen and iron. Heme (protoporphyrin IX) bound to the iron ion is the most abundant and widely used prosthetic group for metalloporphyrins. The heme group is capable of transporting electrons between proteins during respiration, O_2 storing, iron storage and transport. In addition, globin-bound heme acts as sensors during oxygen deprivation (Hoogewijs et al., 2012; Poulos, 2014). Fungi express flavohemoglobins and S-type globins (Vinogradov et al., 2007). Remarkably, fungi of the order Onygenales, such as *Paracoccidioides* spp., express only the S-type globins (sensor globins), which contains a single domain sensor globin (Hoogewijs et al., 2012).

A fungal heme-protein, named fungoglobin (FglA), was identified in *Aspergillus fumigatus* as responsive to low oxygen stress. The *A. fumigatus fglA* transcriptional response occurs during the onset of hypoxic stress. Additionally, FglA was characterized as an important growth regulator, which was confirmed by the *fglA* gene deletion (Hillmann et al., 2014). Therefore, the general aim of this work was to identify and characterize critical elements for the adaptive response to hypoxia, in particular, FglA, in members of the *Paracoccidioides* complex. For the characterization of FglA, molecular dynamics was used to determine the *Paracoccidioides* protein 3D model and its levels of expression during oxygen limitation were evaluated. In addition, FglA function in *Paracoccidioides brasiliensis* was assessed by silencing of this gene, performed via *Agrobacterium tumefaciens*-mediated transformation (ATMT) and antisense RNA technology. A *P. brasiliensis fglA* knockdown strain exhibited growth impairment in hypoxia, corroborating the idea that fungoglobin is important for growth in microaerobic environments. Biochemical test confirms that fungoglobin binds to heme. Initial analyzes were carried out to establish the relationship between FlglA and iron metabolism, as well as during infection. We believe that this molecule may be necessary for the fungal adaptation to infection.

2. Materials and methods

2.1. Ethics statement and mice

This study was conducted in strict accordance with the ethical principles of animal research adopted by the Brazilian Society of Laboratory Animal Science and the Brazilian Federal Law 11,749 (October 2008). The project was approved by institutional Ethics Committee on Animal Use of the Universidade Federal de Goiás (reference number 089/17). Male BALB/c mice, aged 6–8 weeks, were purchased from the Animal house of the Instituto de Patologia Tropical e Saúde Pública – UFG, and were kept in the Animal Facilities in the Laboratório de Biologia Molecular of the Departamento de Bioquímica e Biologia Molecular, Instituto de Ciências Biológicas, Universidade Federal de Goiás.

2.2. In silico analysis

The nucleotide sequence of *fglA* was retrieved from the *Paracoccidioides* spp. genome available at the National Center for Biotechnology Information database (https://www.ncbi.nlm.nih.gov/assembly/?term=Paracoccidioides). This database holds the full genomes of all five *Paracoccidioides* species (*P. lutzii*, *P. brasiliensis*, *P. americana, P. venezuelensis* and *P. restrepiensis*). Globin sequences of the *A. fumigatus* A1163 database (http://www.aspergillusgenome.org), *Ajellomyces dermatitidis* (https://www.ncbi.nlm.nih.gov/assembly/?term=Ajellomyces%20dermatitidis) and *Coccidioides immitis* (https://www.ncbi.nlm.nih.gov/assembly/?term=Coccidioides%20immitis) were downloaded. Online algorithms used to predict protein domains were applied from InterPro [https://www.ebi.ac.uk/interpro/; (Finn et al., 2017)]. The WoLF PSORT [https://www.genscript.com/wolf-psort.html; (Horton et al., 2007)] and the TargetP 1.1 server [http://www.cbs.dtu.dk/services/TargetP/; (Emanuelsson et al., 2007)] were used to predict cell localization. Post-translational O-glycosylation sites were predicted by the NetOGlyc 4.0 Server [http://www.cbs.dtu.dk/services/NetOGlyc/ (Steentoft et al., 2013)]. To determine the identity of the proteins among the species, the Basic Local Alignment Search Tool on NCBI site [BLAST - https://blast.ncbi.nlm.nih.gov/Blast.cgi (Altschul et al., 1990)] was employed. A cladogram was constructed by multiple sequence alignments using CLUSTALX2. The cladogram was generated by the neighbor-joining method and visualized by TreeView software (Page, 1996; Saitou and Nei, 1987; Thompson et al., 1997). Robustness of branches was estimated using 10,000 bootstrapped replicates.

2.3. Protein molecular modeling

A structural model of the putative fungoglobin of *P. brasiliensis* (GenBank accession number XP_010756372.1) was predicted by *in silico* analysis. The amino acid sequence was submitted to homology modeling in the I-TASSER server (Yang et al., 2014; Yang and Zhang, 2016). To determine the architecture of FglA by homology, a crystal structure model was retrieved from the Protein Data Bank, and the TM-score algorithm evaluated the similarities. The COFACTOR (Zhang et al., 2017) and COACH (Yang et al., 2013) algorithms were used to predict functional regions and protein binding sites, respectively. For the structural analysis, the PyMOL molecular visualization program (The PyMOL Molecular Graphics System, Version 2.0 Schrödinger, LLC) was used.

Molecular dynamics (MD) simulation was performed by GROMACS 5.1 software (Pronk et al., 2013) using the AMBER force field (ff99SB-ILDM). For energy minimization, the limit of 1000 kJ/mol was used. For the equilibrium of the thermodynamic variables of the system, simulations of 100 picoseconds of NVT (constant number of particles, volume, and temperature) and 100 picoseconds of NPT (constant number of particles, pressure, and temperature) were performed. Then, the temperature was adjusted by the thermostat to 300 K and maintained throughout the simulation (Pronk et al., 2013). In the NPT simulation, where the volume is allowed to vary, the pressure was maintained by the Parrinello-Rahman barostat (Hutter, 2012). Following these steps, the protein was subjected to the simulation of 100 ns, temperature of 300 K, pressure of 1 atm, and time interval of

2 fs, without conformation restriction. The trajectory was analyzed by the root mean square deviation (RMSD) and the root mean square fluctuation (RMSF) through the gromos algorithm. RMSF is used to verify the fluctuation of amino acid residues of the protein over time. The g_cluster program (GROMACS package) was used to determine the conformations that were present during the simulation, with a cut-off of 0.5 nm to differentiate the conformational sets based on the RMSD profile. We observed the conformational profile of the protein throughout the simulation via cluster analysis (Pronk et al., 2013).

For the analysis of the quality of the generated models, we used the MolProbity server through Ramachandran plots, the general score of the molecule (score molProbity) and the clash score. We compared the structure of the protein before and after the MD with the MolProbity server (Chen et al., 2010).

2.4. Strains and culture conditions

Yeast cells of *P. brasiliensis*, strain 18 (ATCC 32069), *P. lutzii*, strain 01 (ATCC MYA-826), and *P. brasiliensis fglA* silenced strains were used in this work. The cells were maintained in BHI solid medium containing 4% (w/v) glucose for 3 or 5 days at 36 °C and strains were grown in liquid BHI for 72 h at 36 °C. Hypoxia-mimetic conditions were performed as described in Lima and collaborators (Lima et al., 2015). *P. brasiliensis* was submitted to normoxia/hypoxia, and the cells were collected in the time-interval of 5 min to 48 h. For hypoxic conditions, a gas incubator (Multi-Gas Incubator MCO-19 M−UV, Panasonic Biomedical) was used. The oxygen levels were maintained with the set point of 1% O_2, 5% CO_2, and 94% N_2. Normoxic conditions were applied according to general atmospheric levels within the lab (~21% O_2). Depleted iron conditions were obtained according to Parente and contributors (Parente et al., 2011) with modifications. After grown in liquid BHI at 36 °C for 72 h, *P. brasiliensis* yeast cells were transferred to MMcM liquid medium containing 50 μM of the iron chelator bathophenanthroline disulfonate (BPS) or 10 μM of ammonium iron(II) sulfate [$Fe(NH_4)_2(SO_4)_2$] for iron deprivation and control samples, respectively. To prevent protein glycosylation, the fungal cells were cultured in BHI medium containing 50 μM OSMI-1 (Sigma-Aldrich; Jaskiewicz and Townson, 2019) in normoxia and hypoxia for 72 h at 36 °C.

2.5. Gene sequencing

The yeast cells of *P. brasiliensis* and *P. lutzii* were resuspended in STES buffer [0.2 M Tris-HCl pH 7.2, 0.5 M NaCl, 10 mM EDTA, 0.1% (w/v) SDS] supplemented with RNAse (1 μg/mL). Then, the cells were disrupted by vigorous mixing with glass beads in a beadbeater apparatus subjected to three cycles of 30 s at maximum speed. Samples were kept on ice. After lysis, genomic DNA extraction was performed according to standard procedures (Sambrook and Russel, 2001). Oligonucleotides were constructed according to the complete deduced sequence of *fglA* gene (the sequences of the primers are listed in the topic *Expression and purification of recombinant* Pb*FglA*). The gene was amplified by polymerase chain reaction (PCR), using the genomic DNA as template. Amplification was confirmed by visualization of a single PCR product on 1% agarose gel with 665 bp (data not shown). Then, 5 μL of the PCR product was treated with 1 μL of the exonuclease I: shrimp alkaline phosphatase mix (1:9) (GE Healthcare), and incubated at 37 °C for 90 min and a subsequent incubation at 80 °C for 20 min. Thereafter, the sequencing reaction was performed with the BigDye™ reagent (Applied Biosystem™) and the system was subjected to capillary electrophoresis in the automated sequencer ABI 3100 Genetic Analyzer (Applied Biosystem™). The results were analyzed by the software Chromas Lite© 2.1.1 and Clustal X 2.1 (Larkin et al., 2007).

2.6. Yeast cells recovered from infected lung mice: bronchoalveolar samples

P. brasiliensis yeast cells recovered from bronchoalveolar lavage of infected mice were performed according to Pigosso and collaborators (Pigosso et al., 2017). Male BALB/c mice were infected by intranasal administration with 10^5 yeast cells of *P. brasiliensis* in 100 μL of 0.9% (w/v) NaCl saline buffer. After 12 h of infection, the cells were recovered by bronchoalveolar lavage and immediately used for RNA extraction as described below. Control RNA was obtained by incubation of *P. brasiliensis* cells in liquid BHI medium at 37 °C for 12 h.

2.7. RT-qPCR

For all experiments of RT-qPCR, the total RNA was extracted using TRIzol (TRI reagent, Sigma-Aldrich, St. Louis, MO, USA). Samples were treated with DNase (RQ1 RNase-free DNase, Promega) followed by *in vitro* reverse transcription (SuperScript III First-Strand Synthesis Super Mix; Invitrogen, Life Technologies). Oligo(dT) was used for the annealing of the template-primer. cDNAs were submitted to a quantitative real time PCR assay (qPCR) with a SYBR Green PCR Master Mix reagent (Applied Biosystems, Foster City, CA) in a StepOnePlus machine (Applied Biosystems Inc.). Oligonucleotides were designed for the *P. brasiliensis* (*PbfglA*) gene (*PbfglA*-F: 5′-CCATCAATGGCCGTACTATCA-3′; *PbfglA*-R: 5′-GGCTCCATCTTCTTCGGTAAA-3′; GenBank accession number XP_010756372.1). *P. brasiliensis alpha*-tubulin (*Pbtub*-F: 5′-CCCACGAATCCAACTCTGTTAT-3′; *Pbtub*-R: 5′- and GGAGACAGGT TGCCATGTATT-3′; GenBank accession number XP_010763621.1) and *P. brasiliensis* enolase (*Pbeno*-F 5′-GATTTGCAGGTTGTCGCCGA-3′; *Pbeno*-R 5′-TGGCTGCCTGGATGGATTCA-3′ GenBank accession number XM_010761399.1) were used as reference genes. Relative expression levels of genes were calculated using the standard curve method for relative quantification (Bookout et al., 2006). Standard curves were generated by 1/5 dilution of the cDNA solution. Data were expressed as the mean and standard deviation of the biological triplicates of independent experiments. Statistical analysis was performed using the Student's *t*-test and p-values ≤ 0.05 were considered statistically significant.

2.8. Purification and spectrophotometric analysis of recombinant PbFglA

The empty pET-32a vector (Novagen, Madison, WI, USA) was used to construct the pET-32a::*PbfglA* plasmid. The coding sequence of *PbFglA* was amplified with the specific primers *Pb*FglA-F (5′-CGGGATCCATGTCAGCCATCAATGG-3′) and *Pb*FglA-R (5′- GGCGGCCGCTCAATCCAACTCCGGCTTCTCT-3′) and cloned into the *BamH*I-*Not*I sites in the pET-32a vector (*Bam*HI and *Not*I sites are underlined). The transformation of *Escherichia coli* BL21 (DE3) was carried out using standard procedures. Freshly colonies were picked and cultured in LB medium supplemented with ampicillin (0.1 mg/mL). For protein expression, overnight cultured bacteria were first diluted 100-fold in fresh LB medium with ampicillin and cultured with agitation at 37 °C until $O.D._{600}$ ~ 0.6. Isopropyl β-D-1-thiogalactoside (IPTG; Sigma-Aldrich, St Louis, MO, USA) solution was added at a final concentration of 0.5 mM to induce protein expression for 2 h. Bacteria were collected, and soluble proteins were extracted by lysozyme incubation (500 μg/mL) for 2 h, followed by cell sonication. The solubilized material was recovered by centrifugation at 8000*g* for 15 min. Bacterial overexpressed recombinant FglA (rFglA) was purified using Ni_2 + NTA affinity chromatography (Sigma-Aldrich). Protein concentration was determined by the Bradford method (Bradford, 1976) and purity, size, and identity of r*Pb*FglA protein were evaluated using a 12% SDS-PAGE and in-gel protein digestion (Rezende et al., 2011) followed by LC-MS/MS (Lima et al., 2015).

UV–VIS spectra of the recombinant *Pb*FglA was used to determine its biding to hemin. *Pb*FglA and reduced *Pb*FglA (100 μM sodium hydrosulfite, for 1 h at room temperature; Sigma-Aldrich, USA, Ref. N°

71699) was incubated in the absence or presence of 100 μM hemin (Sigma-Aldrich, USA, Ref. N° H9039) for 1 h at room temperature. Absorbances data were recorded in a SpectraMax® Paradigm® Multi-Mode Detection Platform (Molecular Devices, Austria).

2.9. Mice immunization

We used the purified rFglA protein to generate anti-FglA polyclonal antibodies in male BALB/c mice. Mice were immunized by subcutaneous injection of 10 μg of protein (in 50 μL of 1X PBS) with 50 μL of complete Freund's adjuvant in the first immunization. Subsequent injections were maintained with the same sample proportions but with incomplete Freund's adjuvant. Animal was boosted twice at 1-weeks intervals and with the same amount of antigen. One week after the last boost, the serum containing polyclonal antibodies to rFglA was aliquoted and stored at −20 °C. Pre-immune serum was obtained.

2.10. Immunoblotting

Hypoxic and normoxic proteins extracts of *P. brasiliensis* or rFglA protein were loaded (40 μg) on 12% SDS-PAGE. After gel separation, proteins were stained with Coomassie Blue R or transferred to Hybond ECL membrane (GE Healthcare). Subsequently, membranes were incubated with PBS, added 10% (w/v) non-fat milk, and 0.1% (v/v) Tween 20 (PBS-T) for 2 h to block non-specific sites. Then, membranes were incubated with anti-FglA polyclonal antibodies diluted 1:150 in PBS-T for 2 h. Membranes were washed in PBS-T, followed by incubation with phosphatase-conjugated secondary antibody (1:1000) in the dark and at room temperature for 1 h. Labeled detection was carried out using 5-bromo-4-chloro-3-indolylphosphate–nitroblue tetrazolium (BCIP-NBT). Raw Tiff images were analyzed by densitometric analysis of immunoblotting bands using the ImageJ software.

2.11. Construction of *fglA P. brasiliensis* silenced strains by antisense RNA and characterization of mutants

The silencing of *fglA* in *P. brasiliensis* was performed by the antisense RNA technique using an ATMT technology (Almeida et al., 2007; Bailão et al., 2014; Parente-Rocha et al., 2015; Silva et al., 2020). Oligonucleotides were constructed to generate the antisense DNA from *P. brasiliensis* and the fragment of the aRNA oligonucleotide targeting was amplified with the specific primers *asPbfglA-F* (5′CCGCTCGAGCGGCT ATCACCCACATCGATGA3′) and *asPbfglA-R* (5′GGCGCGCCTATGTCCT TGGCTGATTGG 3′) produced a fragment of 119 bp. The *PbfglA* antisense fragment was cloned into the pCR35 plasmid under the control of the CBP-1 (calcium binding protein) promoter from *Histoplasma capsulatum* (Rappleye et al., 2004). After propagating in *E. coli* the cassette containing CBP1 promoter-AS was sub cloned into a pUR-750 plasmid (Torres et al., 2014). A recombinant control was obtained by transformation of *P. brasiliensis* with the empty vector. The *Agrobacterium tumefaciens* strain LBA1100 was cultured in induction medium (IM) at $O.D._{660}$ ~ 0.8 containing antibiotics (kanamycin 100 μg/mL, spectinomycin 250 μg/mL, rifampicin 20 μg/mL, and acetosyringone 0.4 M) and, after that, co-cultivated with *P. brasiliensis* (1:1 and 1:10, ratio). Following this step, transformants were selected in BHI containing hygromycin (Sigma-Aldrich, USA) at 75 μg/mL and randomly selected clones were confirmed for silencing by RT-qPCR.

To characterize the function of FglA in low oxygen concentrations yeast cells of the wild type (WT), those harboring empty vector (EV) and *fglA* silenced strain (*AsFglA*) were cultured in BHI plates at 36 °C for 5 days in normoxia or hypoxic-mimetic conditions, as described above. After this time, the cells were collected for determining viability by staining with 1 μg/mL (w/v) propidium iodide (Sigma-Aldrich, USA). The samples were analyzed in a fluorescence microscope (Zeiss Axiocam MRc – Scope A1).

3. Results and discussion

3.1. Fungoglobins are present in members of the Paracoccidioides complex

Globins are important heme-proteins able to bind to O_2 and thus play an important role in aerobic organisms, acting in processes like respiration, oxidative energy conversion, detoxification of reactive oxygen species and intracellular signaling (Burmester and Hankeln, 2014). Globins also operate as sensors of oxygen levels (Hoogewijs et al., 2012). In the human pathogenic fungus *A. fumigatus*, fungoglobin (*Af*FglA) was described as an important protein for the adaptation to hypoxic stress, which is connected to fungal growth (Hillmann et al., 2014). Several proteins are regulated in *Paracoccidioides* spp. in response to hypoxia (Lima et al., 2015), and the characterization of the *Paracoccidioides* FglA protein has not been established yet. Therefore, we sought to identify a putative globin-hypoxic responsive protein, FglA, in members of the *Paracoccidioides* genus. The sequence of the *Af*FglA gene (GenBank accession number AFUB_004020) contains 282 aa and was searched against the genomic database of *Paracoccidioides* spp. As a result, we identified a homologous gene in *P. brasiliensis* - *Pb*18 (GenBank accession number XP_010756372.1), *P. americana* - *Pa*03 (GenBank accession number EEH19835.1,), *P. venezuelensis* - *Pv*300 (GenBank accession number ODH38897.1), *P. restrepiensis* - *Pr*CNH (GenBank accession number ODH50562.1), but not in *P. lutzii* - *Pl*01 (Fig. 1A). The analysis revealed 27% identity on the amino acid level with *Af*FglA, although structural similarity with protoglobin from *Anaeromybacter* sp. was predicted to be 70%, as shown below. Then, the deduced amino acid sequences of the protein and their domains were characterized. The InterPro search revealed the presence of protoglobin domains (Pfam family number PF11563; Fig. 1A), which consists of a single globin domain conserved from Archaea (Nardini et al., 2008). It has been noted that domains of the protoglobin family are part of the superfamily of hemoglobins and they act as an oxygen level sensor granting the access of O_2 to the heme by apolar tunnels (Nardini et al., 2008; Zhang and Phillips, 2003). Interestingly, the amino acid histidine (H in Fig. 1A) is conserved among species and possibly acts as an anchor for the heme prosthetic group (Frausto da Silva and Williams, 2001; Kaim et al., 2013).

Previous phylogenetic analysis of genomes of 165 fungi species identified putative globins and revealed the presence of S-globin only in the *P. americana* species (Hoogewijs et al., 2012). Through a detailed analysis, we identified the genomic sequence in four out of five species of the *Paracoccidioides* genus. Ascomycetes, Onygenales and Pezizomycetes do not express flavohemoglobins. Instead, they code only for sensor-type globins (Hoogewijs et al., 2012). Due to the presence of S-globins in *P. brasiliensis*, *P. venezuelensis* and *P. restrepiensis*, we carried out a comprehensive survey of Onygenales protein phylogenetic relationships, including *P. americana*, *P. brasiliensis*, *P. venezuelensis*, *P. restrepiensis*, *A. dermatitidis*, *C. immitis* and *A. fumigatus* as outgroup belonging to the Eurotiales order (Fig. 1B). These results highlight the evolutionary similarities among *Paracoccidioides* species, as well as the globins of fungi belonging to the Onygenales order.

Subsequently, in order to verify the presence/absence of the *fglA* gene in *P. lutzii*, oligonucleotide primers were constructed using the complete *P. brasiliensis-fglA* (*PbfglA*) gene as a template, and the PCR reaction was performed with *P. lutzii* gDNA as template. The result pointed to a DNA fragment in *P. lutzii* of identical size to *P. brasiliensis fglA* (an amplicon of 665 base pairs) (data not shown). Then, the PCR products were subjected to DNA sequencing. Sequence alignment (Supplementary Fig. 1) demonstrated that the genes were identical between the two *Paracoccidioides* species. Furthermore, the deduced *P. lutzii* amino acid sequence contains the conserved protoglobin domain and the histidine residue, like the other *Paracoccidioides* species. The GenBank accession number of the gene reported here is MK895509.

The *P. brasiliensis* FglA amino acid sequence was submitted to several algorithms in order to predict the protein subcellular localization.

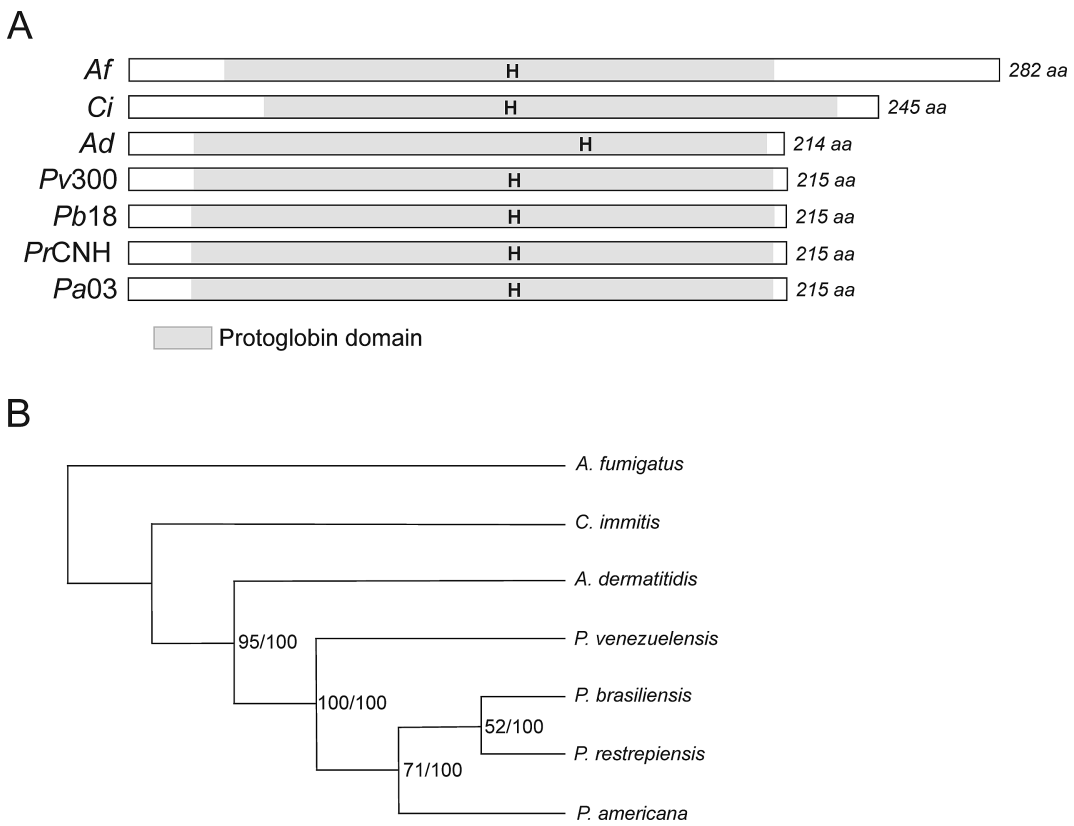

Fig. 1. Alignment and phylogenetic analysis **of the *fglA* gene. (A)** Sequences from *Paracoccidioides* spp. (*P. venezuelensis*- *Pv*300 - ODH38897.1, *P. brasiliensis* - *Pb*18 - XP_010756372.1, *P. restrepiensis* – *Pr*CNH - ODH50562.1, *P. americana* - *Pa*03 - EEH19835.1), *A. dermatitidis* - *Ad* - XP_002625170.1, *C. immitis* - *Ci*- XP_001244432.1 and *A. fumigatus*- *Af* - AFUB_004020 were used. The domains of protoglobin (Pfam family number PF11563) are featured in light gray. "H" indicates a putative histidine residue capable of binding to the heme group. **(B)** Cladogram comparing the FglA amino acid sequences of *Paracoccidioides* spp., *A. dermatitidis*, *C. immitis*, and *A. fumigatus*. Neighbor joining tree was used for displaying phylogenetic tree. The numbers above branches indicate bootstrap support values of neighbor joining (bootstrap repeat is 10,000).

Results suggested that FglA is cytoplasmatic (data not shown). Regarding the Gene Ontology (GO) classification, we obtained information that *Pb*FglA participates in biological process, such as oxygen transport (GO: 0015671) and molecular functions related to heme (GO: 0020037), oxygen (GO: 0019825) and iron-binding (GO: 0005506).

3.2. Molecular modeling of P. brasiliensis fungoglobin a (PbFglA) predict its interaction with heme and oxygen

Initially, we aimed to characterize the three-dimensional structure of *Pb*FglA. The PDBID:5ohe crystal of *Anaeromyxobacter* sp. Fw109-5 (Fig. 2) was used as a structure model. We obtained a TM-score of 0.71 (SD ± 0.12) for the *Pb*FglA predicted structure. According to the COFACTOR and COACH algorithms, the modeled protein presented the heme group as the primary ligand (70% of confidence); it was possible to identify the heme binding site (Fig. 2A). The *Pb*FglA model was predicted to have molecular function of heme- and oxygen-binding (88% of confidence), biological process related to oxygen transport (88% of confidence) and responsiveness to chemical stimuli (58% of confidence).

Molecular dynamics was performed to correct possible errors in the predicted structure. Supplementary Fig. 2 evidences the quality of the molecular dynamics. The Ramachandram plot (Supplementary Fig. 2A) showed 81.2% of amino acid residues in favorable regions and 91.1% in allowed regions before molecular dynamics simulation. Supplementary Fig. 2B shows that after molecular dynamics 92.5% of the residues were in favorable regions and 98.6% in allowed regions. These results indicate an improvement of the predicted protein structure. Supplementary Fig. 2C shows the cluster plot with the most representative conformational groups at each time-step of the simulation. We found 3 main clusters along the molecular dynamic's trajectory. In Supplementary Fig. 2D, the RMSD plot shows the mean deviation of the initial-time structure until the final time of the simulation, disregarding hydrogen atoms. RMSF plot (Supplementary Fig. 2E) shows the residues that were most flexible along the molecular dynamics (peaks in the graph), and in Supplementary Fig. 2F, the flexible regions are highlighted in red. The molecular dynamics increased confidence in the prediction of the three-dimensional structure of *Pb*FglA.

Molecular dynamics resulted in a refined *Pb*FglA structure (Fig. 2A). A detailed analysis of the amino acids showed significant similarities between the 5hoe crystal and *Pb*FglA, highlighting important characteristics of the structure and its function. *Pb*FglA amino acid residue HIS137 is predict as an anchor for heme binding (Fig. 2B). This residue is conserved in the 5hoe crystal (HIS99), as predicted in the sequence analyzes shown in Fig. 1A. This data is supported by structural analyzes of heme proteins available in the PDB (Protein Data Bank) that revealed that cysteine, histidine, phenylalanine, methionine, and tyrosine as the most frequent residues in heme anchorage (Li et al., 2011). Remarkably, the heme group binds to histidine more frequently (Li et al., 2011), and the presence of histidine as an anchor is an intrinsic feature of globins (Frausto da Silva and Williams, 2001; Kaim et al., 2013). In addition, the amino acid residues of the 5ohe crystal VAL98 and ILE95 that correspond to the amino acids VAL133 and ILE136 of the fungoglobin model possibly assist in the stability of the molecule binding to Fe(II), as represented in the Fig. 2B. The analysis showed the *Pb*FglA tyrosine residue (TYR60) that potentially acts by interacting with the oxygen molecule (Fig. 2C). This residue is related to the uptake,

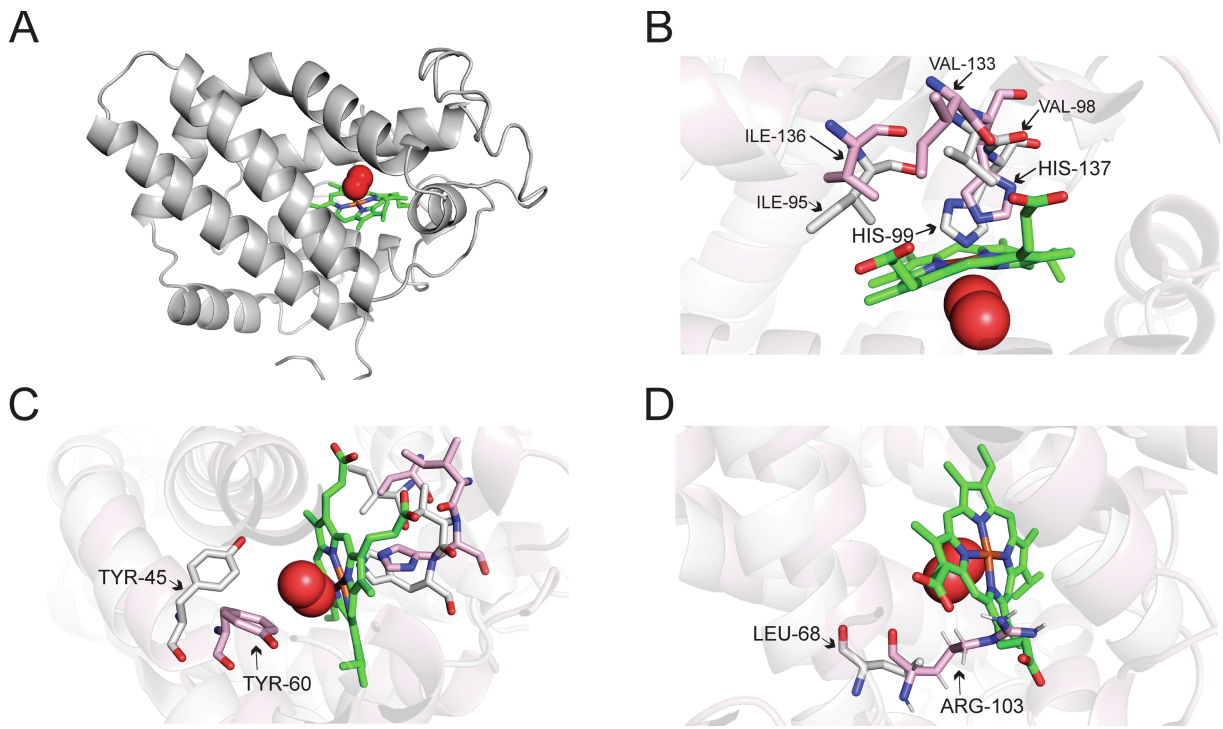

Fig. 2. Modeling the predicted FglA. (A) *P. brasiliensis* fungoglobin patterned by homology (gray), with the heme group (green) and the oxygen atom O_2 (red) in the probable binding site. **(B)** Amino acid residues involved in the interaction with the heme group. The HIS137 is the key residue in the interaction with the iron of the heme group. **(C)** Site of the interaction of the heme group. The amino acid TYR45 (5ohe) and TYR60 (*Pb*FglA) are responsible for the interaction with oxygen. **(D)** Amino acids LEU68 (5ohe) and ARG103 (*Pb*FglA) control the entry and exit of the heme group.

stabilization and permanence of the oxygen connected to the heme molecule - mutation in this amino acid in *Anaeromyxobacter* sp. Fw109-5 prevents oxygen uptake (Nardini et al., 2008; Stranava et al., 2017). Another important finding was that *Pb*FglA ARG103 acts similarly to the 5ohe crystal LEU68, potentially controlling the entry and exit of the heme group within globular protein structures (Fig. 2D) (Stranava et al., 2017).

3.3. *FglA recombinant protein and polyclonal antibodies production allowed the identification of FglA in the fungus proteome*

To produce the FglA recombinant protein (rFglA) and polyclonal antibodies, the FglA was expressed in *E. coli*. The overproduction of the recombinant protein fused to TrxA in bacteria and its purification were carried out (Supplementary Fig. 3A). The rFglA was injected into male BALB/c mice for polyclonal antibodies production (Supplementary Fig. 3B). Analysis of the MS/MS spectra confirmed the expression of FglA (Supplementary Fig. 4, Supplementary Table 1). The molecular mass of the native FglA was 60 kDa, higher than that of the predicted protein, which was 25 kDa (Supplementary Fig. 5A). In this way, we searched for post-translational modifications by using online algorithms and we found three O-glycosylation sites for FglA. To verify the glycosylation effect on the molecular mass of the native FglA, we cultured *P. brasiliensis* in an environment that inhibits general protein O-glycosylation using OSMI-1 (Jaskiewicz and Townson, 2019). To verify the effects of OSMI-1 on *P. brasiliensis* growth, the yeast cells were grown in liquid BHI for 72 h at 36 °C in 96-weel plate and their viability was determined using a 0.02% resazurin solution (data not shown). Immunoblotting confirmed the O-glycosylation and the predicted molecular size with or without glycosylation, revealing FglA with molecular sizes of 60 and 25 kDa, respectively (Supplementary Fig. 5A and 5B).

3.4. *O_2 influences PbFglA levels*

Yeast cells of *P. brasiliensis* were subjected to normoxic and hypoxic environments to quantify the expression of the *PbfglA* in oxygen-limiting conditions through RT-qPCR. The RNAs were extracted from yeast cells in normoxia and hypoxia during early and late times (5 min, 15 min, 30 min, 1 h, 2 h, 4 h, 6 h, 9 h, and 12 h). Fig. 3A shows that *fglA* expression is regulated by hypoxia after 1 h of treatment (p-value $\leq$ 0.01 and fold $\geq$ 1.5) and remains upregulated upon oxygen limitation. The transcriptional response of *fglA* occurs within the first 15 min of hypoxic stress in *A. fumigatus* (Hillmann et al., 2014). In addition, the *Pb*FglA levels were analyzed by immunoblot assay using anti-FglA polyclonal antibodies. Data show that in hypoxia at 12, 24, and 48 h the accumulation of *Pb*FglA was higher than in normoxia (Fig. 3B). The increased protein accumulation indicates that FglA effectively participates in oxygen deprivation adaptation. Protein levels of FglA increase over time also in normoxia (Fig. 3B), suggesting additional regulatory mechanisms other than oxygen levels. The observed increase also in normoxia is possibly due to the simultaneous response to different stimuli. Since FglA is predicted to bind heme, the most likely is that iron content could be the responsible for this behavior. Scientific evidences of that relationship between FglA and iron is discussed in topic below.

To continue the investigation, *P. brasiliensis* yeast cells were submitted to re-oxygenation. For this, yeast cells were incubated up to 4 h in oxygen-limiting conditions followed by re-oxygenation and incubation for 4 additional hours. Control cells were submitted to normoxia. Fig. 4 shows that the *fglA* transcript was 2-fold induced during hypoxia (until 240 min). When cells were re-oxygenated (~21% O_2), this overexpression remained during the first 2 h (2-fold, time point 360 min) but then decreased to levels found during normoxia. This result demonstrates that *Pb*FglA expression is oxygen dependent with increase or decrease in expression according to its availability. Altogether, these data suggest an important role of the FglA in response to

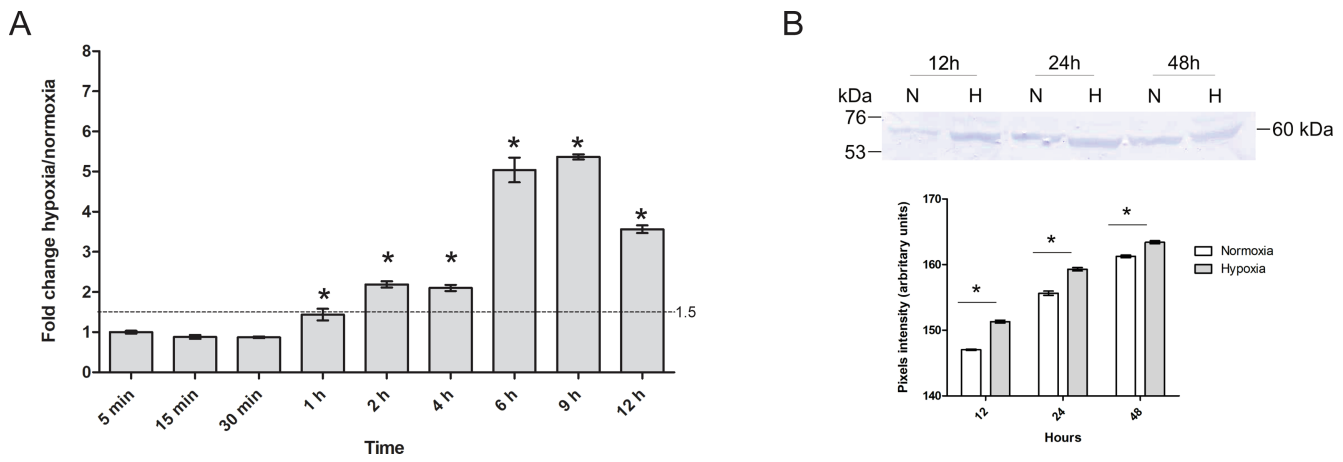

Fig. 3. Fungoglobin transcript and protein expression in *P. brasiliensis* under hypoxia. **(A)** Kinetics of the *fglA* transcript expression during hypoxia determined by RT-qPCR. The student's *t*-test was used to determine the level of significance, where "*" indicates differentially significant expression ($p \leq 0.01$) among three biological replicates. The dotted line represents 1.5 fold. **(B)** Protein levels of FglA during hypoxia determined by western blot assay. The native FglA shows a molecular mass of 60 kDa. The Student's *t*-test was used to determine the level of significance, where "*" indicates differentially significant expression ($p \leq 0.01$). Raw Tiff images were analyzed by densitometric analysis of immunoblotting bands using the ImageJ software.

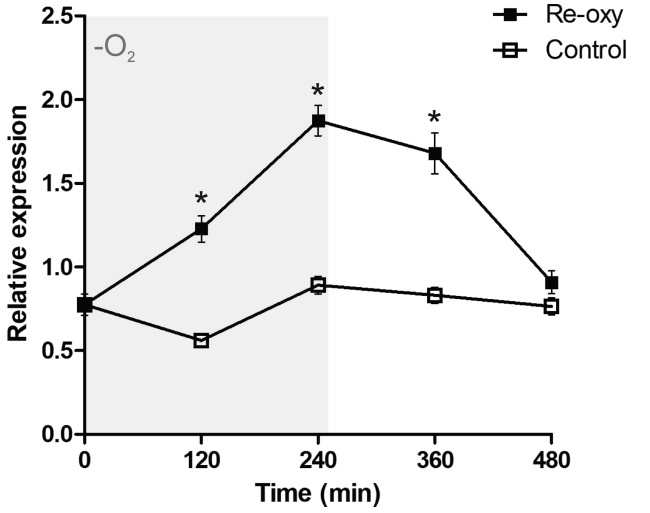

Fig. 4. O_2-dependent gene expression of *P. brasiliensis fglA*. The graphs display the kinetics of *PbfglA* expression during the re-oxygenation of the environment determined by RT-qPCR. Three independent replicates were performed. Student's *t*-test was used to determine the level of significance, where "*" indicates differentially significant expression ($p \leq 0.01$). The data were normalized using the constitutive gene encoding *alpha*-tubulin (GenBank accession number XP_010763621.1) as reference.

hypoxia.

3.5. Fungoglobin deficiency promotes reduction in yeast cells growth in low-oxygen environments

According to results above, *PbfglA* is regulated during the lack of O_2. To demonstrate the effects of FglA in *P. brasiliensis* cell biology, we obtained mutant strains by the antisense RNA technology. The method provided FglA-knocked-down strains in *P. brasiliensis* yeast cells, as demonstrated by RT-qPCR (Fig. 5A). We selected a 62% silenced strain, as demonstrated by RT-qPCR of yeast cells in hypoxia, (Fig. 5A). The silenced strain presented a 62% level of transcript expression in hypoxia, compared to normoxia. Indeed, the hypoxia sensitive phenotypes were visible at low O_2 concentration in silenced strains as compared to WT and to the Empty Vector (EV), as depicted in Fig. 5B. As a result, growth was visually affected in silenced strains of *P. brasiliensis*, indicating that FglA is fundamental for the development of the fungus in hypoxia. Viability analysis was performed at 5 days-point of growth and reveals that most cells remains viable (Supplementary Fig. 6). This result reinforces that the growth defect is linked to FglA deficiency and not to cell death. Similar results were found in *A. fumigatus* in which strains deleted for FglA presented lower growth in hypoxic environments (Hillmann et al., 2014).

3.6. PbFglA is an iron responsive

After checking the hypoxia response profile, initial analyzes were carried out to investigate the relationship of FglA with iron ion. Immunobloting analyzes during nomoxia/hypoxia (Fig. 3B) showed an increase in the levels of FglA in normoxia, suggesting that the protein not only responds to oxygen levels, but also to other elements. Our hypothesis was that FglA is responsive to iron since heme/hemeproteins may be a major connector between the availability of oxygen and iron metabolism by interacting with both elements. The predicted heme-binding site was conserved in *Pb*18 as demonstrated by *in silico* analyzes (Figs. 1 and 2) and, therefore, we first checked experimentally the heme binding capacity of this protein. Spectrophotometric analyzes were performed and the UV–VIS spectrum from recombinant purified protein exhibited an absorbance profile like that of purified hemin (Fig. 6A). When reduced, FglA does not bind to hemin. Likewise, in *A. fumigatus*, fungoglobin has the capacity to bind to hemin (Hillmann et al., 2014). Bacteria and fungi can use hemin as a sole source of iron for growth (Desai et al., 1995; Foster, 2002), just like *Paracoccidioides* (Bailão et al., 2014).

In addition, RT-qPCR was performed to quantify the *PbfglA* transcript levels during iron deprivation to verify the relationship of *fglA* and iron availability. *PbfglA* was upregulated during the first 6 h of iron depletion, suggesting a role of this protein during this stress condition (Fig. 6B). An important host defense strategy is to limit the availability of iron to extracellular pathogens by intracellular sequestration (Ganz, 2009), *Paracoccidioides* can survive iron deprivation (Parente et al., 2011). The suggestion that fungoglobin can obtain iron from heme must be investigated in future works. In contrast, the transcriptional expression of *PbfglA* decreased at 12 and 24 h (Fig. 6B). We believe that at later times other mechanisms of iron metabolism are more active, such as hemoglobin uptake (Bailão et al., 2014), expression of siderophores (Silva et al., 2020; Silva-Bailão et al., 2014) or activation of the reductive pathway (Bailão et al., 2015). These mechanisms have been reported to occur in the *Paracoccidioides* genus.

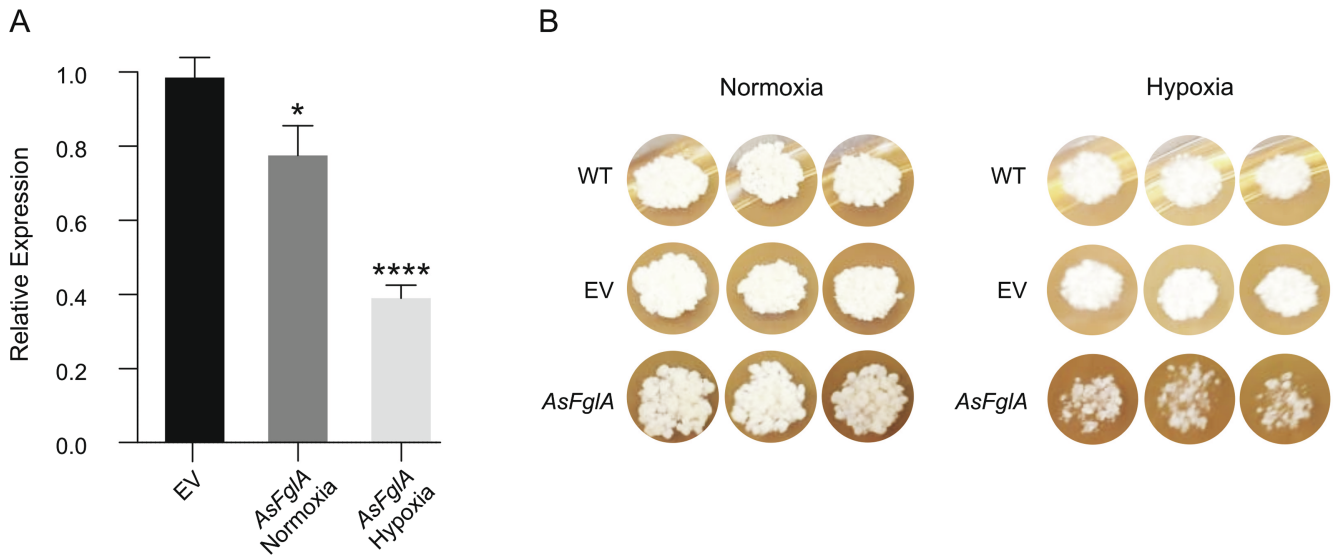

Fig. 5. *P. brasiliensis* silencing of *fglA* gene via *A. tumefaciens*-mediated transformation (ATMT). A) Relative quantification performed by RT-qPCR of silencing level with *Pb*FglA-aRNA cultured in normoxia and hypoxic-mimetic conditions. The transcript level of *Pb*WT transformed with the empty vector (EV) was also quantified and used as control. The enolase gene (GenBank accession number XM_010761399.1) was used as the reference. The Student's *t*-test was used for statistical comparisons. * $p < 0.05$ and **** $p < 0.0005$. The graph shows an average representation of the EV under normoxia and hypoxia. Results were not statistically significant. **B)** Cells of *P. brasiliensis* (WT), EV and the silenced clone for FglA (*AsFglA*) were collected at density of 10^6 cells and spotted on the plate with solid BHI media, followed by culturing in normoxia and hypoxia for 5 days.

3.7. Fungoglobin transcription is upregulated in P. brasiliensis during murine lungs infection

Paracoccidioides spp. faces several adverse conditions in host and can adapt to them as demonstrated *in vitro* and *in vivo* (Camacho and Niño-Vega, 2017; Chaves et al., 2017, 2019; de Curcio et al., 2017; Grossklaus et al., 2013; Lima et al., 2014, 2015, Parente et al., 2011, 2013, 2015; Parente-Rocha et al., 2015; Pigosso et al., 2017; Portis et al., 2020; Rodrigues et al., 2016). Pulmonary concentrations of oxygen and iron may influence the onset of infection, and we hypothesize that fungoglobin may play a role in the survival of the fungus. In lung oxygen levels are lower than atmospheric levels (Carreau et al., 2011; Grahl et al., 2011; Grahl and Cramer, 2010) and iron supply directly influence the inflammatory and infections process (Zhang et al., 2019). It is known that, at the first 6 h of intranasal inhalation, *Paracoccidioides* cells are able to establish pulmonary infection (Pigosso et al., 2017). Thus, we decided to verify whether *fglA* is induced in *P. brasiliensis* during murine lung infection. To evaluate the expression of *fglA* in an *in vivo* model, we infected male BALB/c mice with viable *P. brasiliensis* yeast cells. After 12 h of intranasal infection, we performed bronchoalveolar lavage recovering the fungi. As depicted in Fig. 7, the levels of *fglA* transcript were increased approximately 3-fold in yeast cells infecting mice lungs. This finding suggests that during the onset of the infectious process FglA can be activated by both, oxygen, and iron levels. This hypothesis could be reinforced, considering that *in vitro* tests at 6 h show *fglA* transcript increase of approximately 5-fold during

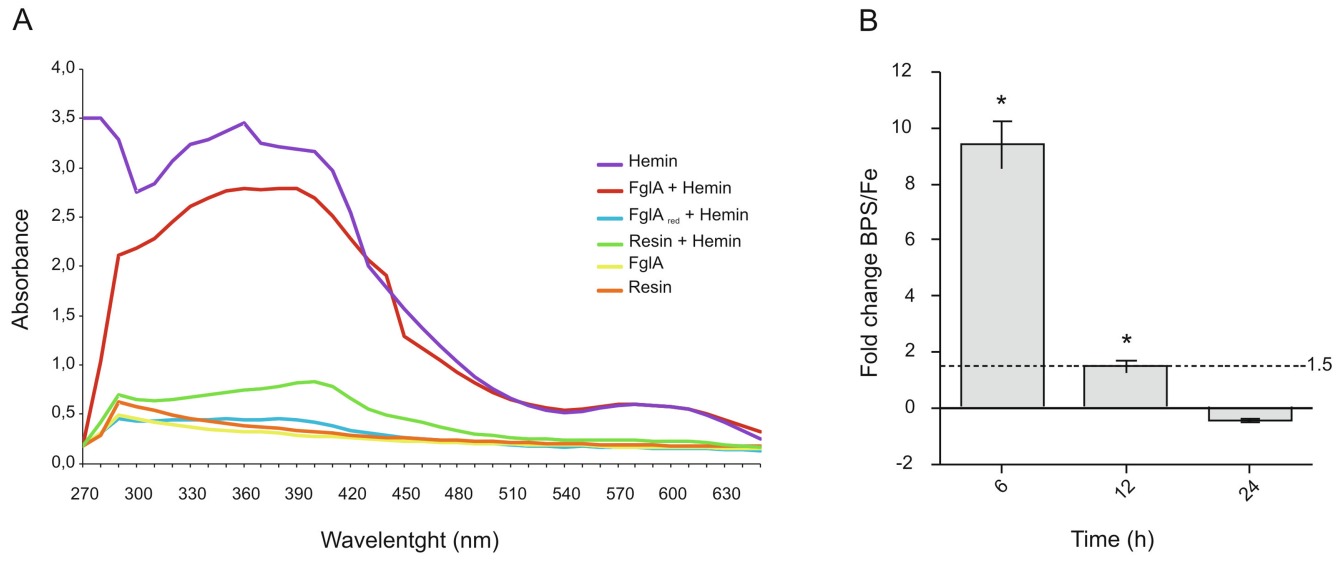

Fig. 6. Fungoglobin is a heme-protein and responds to iron. (A) Absorbance spectra from purified recombinant FglA in the oxidized (red) and reduced state (blue) following addition of hemin. Controls were obtained: oxidized hemin (purple), only FglA (yellow), resin (orange) and resin plus hemin (green). **(B)** Kinetics of *PbfglA* expression in iron deprivation determined by RT-qPCR. The Student 's *t*-test was used to determine the level of significance, where "*" indicates differentially significant expression ($p \leq 0.01$). The dotted line represents 1.5-fold.

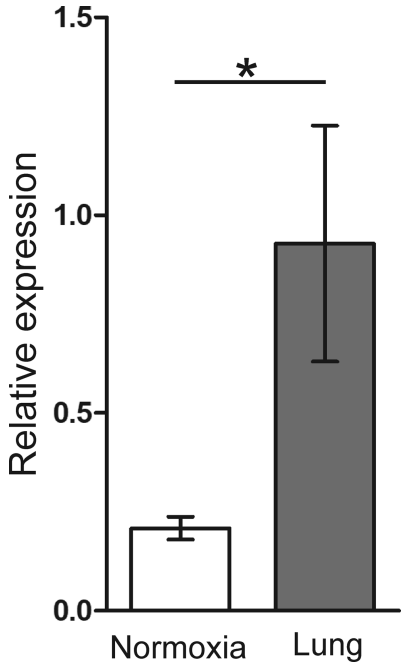

Fig. 7. Expression of *fglA* in *P. brasiliensis* yeast cells recovered from lung of infected mice. RT-qPCR determined the *PbfglA* expression during mice pulmonary infection. *P. brasiliensis* yeast cells were injected in mice by intranasal administration and recovered after 12 h by broncoaveolar lavage. The Student's *t*-test was used to determine the level of significance, where "*" indicates differentially significant expression ($p \leq 0.01$). The data were normalized using the constitutive gene encoding *alpha*-tubulin (GenBank accession number XP_010763621.1) as the reference.

hypoxia (Fig. 3A) and around 10-fold in iron deprivation (Fig. 6B). Low oxygen levels are found during fungal infections (Grahl et al., 2012; Grahl and Cramer, 2010) reaching concentrations below 1% (Grahl et al., 2011) and levels of iron increase the susceptibility of mice to infection by *P. brasiliensis* (Parente et al., 2011). Taking into account that *Paracoccidioides* survives to hypoxia (Lima et al., 2015) and iron starvation (Parente et al., 2011), possibly fungoglobin can play an important role in the pathophysiology of the *Paracoccidioides* spp. disease.

4. Conclusions

Decreasing oxygen to critical levels induces *Paracoccidioides* spp. to establish strategies for survival. In this work, we demonstrated that a fungoglobin of *P. brasiliensis*, FglA, is prominently expressed upon hypoxia, suggesting that this protein presents a role in oxygen limiting conditions. In addition, the relationship between FglA and iron metabolism was initially evidenced. In a murine pulmonary PCM, the transcript increased. In agreement to the significance of this protein in oxygen deprivation, we demonstrated that a strain silenced for the gene presented growth impairment in hypoxic conditions. Altogether, the results showed the relevance of the *Paracoccidioides* spp. fungoglobin protein to its pathophysiology.

CRediT authorship contribution statement

Lucas Nojosa Oliveira: Conceptualization, Methodology, Formal analysis, Validation, Investigation, Data curation, Writing - original draft, Writing - review & editing. **Relber Aguiar Gonçales:** Methodology, Validation, Investigation. **Marielle Garcia Silva:** Methodology, Formal analysis, Validation. **Raisa Melo Lima:** Methodology, Software, Validation, Writing - original draft. **Mariana Vieira Tomazett:** Methodology, Formal analysis, Validation. **Juliana Santana de Curcio:** Methodology, Formal analysis, Validation, Writing - original draft. **Juliano Domiraci Paccez:** Methodology, Validation. **Vanessa Rafaela Milhomem Cruz-Leite:** Methodology, Formal analysis, Validation. **Fernando Rodrigues:** Data curation. **Patrícia de Sousa Lima:** Methodology, Investigation, Data curation, Writing - review & editing. **Maristela Pereira:** Data curation. **Célia Maria de Almeida Soares:** Conceptualization, Investigation, Data curation, Funding acquisition, Resources, Project administration, Supervision, Writing - original draft, Writing - review & editing.

Declaration of Competing Interest

All authors declare that there is no conflict of interest.

Acknowledgments

This work at Universidade Federal de Goiás funded by grants from National Institute of Host-Parasite Interaction (HPI), Fundação de Amparo à Pesquisa do Estado de Goiás – FAPEG, and Conselho Nacional de Desenvolvimento Científico e Tecnológico – CNPq. CMAS and MP are fellow researchers from CNPq. LNO is fellow researcher from Faculdade Estácio de Goiás (DPE – CI 013/2020). LNO and RML were supported by fellowships from Coordenação de Aperfeiçoamento de Pessoal de Nível Superior - CAPES. MGS was supported by CNPq. MVT was supported by a fellowship from FAPEG. RAG was supported by Coordenação de Aperfeiçoamento de Pessoal de Nível Superior (CAPES; grant: 88887.333726/2019-00). FR was supported by the Northern Portugal Regional Operational Programme (NORTE 2020), under the Portugal 2020 Partnership Agreement, through the European Regional Development Fund (FEDER) (NORTE-01-0145-FEDER-000013). We are grateful to Mariana Pires de Campos Telles and Thais Guimarães de Castro for helping in DNA sequencing. The authors also wish to thank Santiago Aguiar Espellet Soares for the technical assistance.

Appendix A. Supplementary material

Supplementary data to this article can be found online at https://doi.org/10.1016/j.fgb.2020.103446.

References

Almeida, A.J., Carmona, J.A., Cunha, C., Carvalho, A., Rappleye, C.A., Goldman, W.E., Hooykaas, P.J., Leão, C., Ludovico, P., Rodrigues, F., 2007. Towards a molecular genetic system for the pathogenic fungus *Paracoccidioides brasiliensis*. Fungal Genet. Biol. 44, 1387–1398. https://doi.org/10.1016/j.fgb.2007.04.004.

Altschul, S.F., Gish, W., Miller, W., Myers, E.W., Lipman, D.J., 1990. Basic local alignment search tool. J. Mol. Biol. 215, 403–410. https://doi.org/10.1016/S0022-2836(05)80360-2.

Arnold, F., West, D., Kumar, S., 1987. Wound healing: the effect of macrophage and tumour derived angiogenesis factors on skin graft vascularization. British J. Exp. Pathol. 68, 569–574.

Bagagli, E., Theodoro, R.C., Bosco, S.M.G., McEwen, J.G., 2008. *Paracoccidioides brasiliensis*: Phylogenetic and ecological aspects. Mycopathologia 165, 197–207. https://doi.org/10.1007/s11046-007-9050-7.

Bailão, E.F.L.C., de Lima, P.S., Silva-Bailão, M.G., Bailão, A.M., da Fernandes, G.R., Kosman, D.J., de Soares, C.M.A., 2015. *Paracoccidioides* spp. ferrous and ferric iron assimilation pathways. Front. Microbiol. 6, 1–12. https://doi.org/10.3389/fmicb.2015.00821.

Bailão, E.F.L.C., Parente, J.A., Pigosso, L.L., de Castro, K.P., Fonseca, F.L., Silva-Bailão, M.G., Báo, S.N., Bailão, A.M., Rodrigues, M.L., Hernandez, O., McEwen, J.G., de Soares, C.M.A., 2014. Hemoglobin Uptake by *Paracoccidioides* spp. Is Receptor-Mediated. PLoS Neglected Tropical Diseases 8, 1–20. https://doi.org/10.1371/journal.pntd.0002856.

Blatzer, M., Barker, B.M., Willger, S.D., Beckmann, N., Blosser, S.J., Cornish, E.J., Mazurie, A., Grahl, N., Haas, H., Cramer, R.A., 2011. SREBP Coordinates Iron and Ergosterol Homeostasis to Mediate Triazole Drug and Hypoxia Responses in the Human Fungal Pathogen *Aspergillus fumigatus*. PLoS Genet. 7, e1002374. https://doi.org/10.1371/journal.pgen.1002374.

Bookout, A.L., Cummins, C.L., Mangelsdorf, D.J., Pesola, J.M., Kramer, M.F., 2006. High-Throughput Real-Time Quantitative Reverse Transcription PCR. p. Unit 15.8. In: Current Protocols in Molecular Biology. John Wiley & Sons Inc, NJ, USA. https://doi.org/10.1002/0471142727.mb1508s73.

Bradford, M.M., 1976. A rapid and sensitive method for the quantitation of microgram quantities of protein utilizing the principle of protein-dye binding. Anal. Biochem. 72,

248–254.
Brummer, E., Castaneda, E., Restrepo, A., 1993. Paracoccidioidomycosis: An update. Clin. Microbiol. Rev. 6, 89–117. https://doi.org/10.1128/CMR.6.2.89.Updated.
Burmester, T., Hankeln, T., 2014. Function and evolution of vertebrate globins. Acta Physiol. 211, 501–514. https://doi.org/10.1111/apha.12312.
Camacho, E., Niño-Vega, G.A., 2017. *Paracoccidioides* Spp.: Virulence Factors and Immune-Evasion Strategies. Mediators Inflamm. 2017, 5313691. https://doi.org/10.1155/2017/5313691.
Carreau, A., Hafny-Rahbi, B.El, Matejuk, A., Grillon, C., Kieda, C., 2011. Why is the partial oxygen pressure of human tissues a crucial parameter? Small molecules and hypoxia. J. Cell Mol. Med. 15, 1239–1253. https://doi.org/10.1111/j.1582-4934.2011.01258.x.
Chang, Y.C., Bien, C.M., Lee, H., Espenshade, P.J., Kwon-Chung, K.J., 2007. Sre1p, a regulator of oxygen sensing and sterol homeostasis, is required for virulence in *Cryptococcus neoformans*. Mol. Microbiol. 64, 614–629. https://doi.org/10.1111/j.1365-2958.2007.05676.x.
Chaves, A.F.A.A., Castilho, D.G., Navarro, M.V., Oliveira, A.K., Serrano, S.M.T.T., Tashima, A.K., Batista, W.L., 2017. Phosphosite-specific regulation of the oxidative-stress response of *Paracoccidioides brasiliensis*: a shotgun phosphoproteomic analysis. Microbes Infect. 19, 34–46. https://doi.org/10.1016/j.micinf.2016.08.004.
Chaves, E.G.A., Parente-Rocha, J.A., Baeza, L.C., Araújo, D.S., Borges, C.L., de Oliveira, M.A.P., de Soares, C.M.A., 2019. Proteomic Analysis of *Paracoccidioides brasiliensis* During Infection of Alveolar Macrophages Primed or Not by Interferon-Gamma. Front. Microbiol. 10. https://doi.org/10.3389/fmicb.2019.00096.
Chen, V.B., Arendall, W.B., Headd, J.J., Keedy, D.A., Immormino, R.M., Kapral, G.J., Murray, L.W., Richardson, J.S., Richardson, D.C., 2010. MolProbity: All-atom structure validation for macromolecular crystallography. Acta Crystallogr. D Biol. Crystallogr. 66, 12–21. https://doi.org/10.1107/S0907444909042073.
de Curcio, J.S., Silva, M.G., Silva Bailão, M.G., Báo, S.N., Casaletti, L., Bailão, A.M., de Almeida Soares, C.M., 2017. Identification of membrane proteome of *Paracoccidioides lutzii* and its regulation by zinc. Future Sci. OA 3, FSO232. https://doi.org/10.4155/fsoa-2017-0044.
Desai, P.J., Nzeribe, R., Genco, C.A., 1995. Binding and accumulation of hemin in *Neisseria gonorrhoeae*. Infect. Immun. 63, 4634–4641.
Dewhirst, M.W., 1998. Concepts of oxygen transport at the microcirculatory level. Seminars in Radiation Oncol. 8, 143–150.
Dubois, J.C., Smulian, A.G., 2016. Sterol Regulatory Element Binding Protein (Srb1) Is Required for Hypoxic Adaptation and Virulence in the Dimorphic Fungus Histoplasma capsulatum 1–19. https://doi.org/10.1371/journal.pone.0163849.
Emanuelsson, O., Brunak, S., von Heijne, G., Nielsen, H., 2007. Locating proteins in the cell using TargetP, SignalP and related tools. Nat. Protoc. 2, 953–971. https://doi.org/10.1038/nprot.2007.131.
Finn, R.D., Attwood, T.K., Babbitt, P.C., Bateman, A., Bork, P., Bridge, A.J., Chang, H.Y., Dosztanyi, Z., El-Gebali, S., Fraser, M., Gough, J., Haft, D., Holliday, G.L., Huang, H., Huang, X., Letunic, I., Lopez, R., Lu, S., Marchler-Bauer, A., Mi, H., Mistry, J., Natale, D.A., Necci, M., Nuka, G., Orengo, C.A., Park, Y., Pesseat, S., Piovesan, D., Potter, S.C., Rawlings, N.D., Redaschi, N., Richardson, L., Rivoire, C., Sangrador-Vegas, A., Sigrist, C., Sillitoe, I., Smithers, B., Squizzato, S., Sutton, G., Thanki, N., Thomas, P.D., Tosatto, S.C.E., Wu, C.H., Xenarios, I., Yeh, L.S., Young, S.Y., Mitchell, A.L., 2017. InterPro in 2017-beyond protein family and domain annotations. Nucleic Acids Res. 45, D190–D199. https://doi.org/10.1093/nar/gkw1107.
Fortes, M.R.P., Miot, H.A., Kurokawa, C.S., Marques, M.E.A., Marques, S.A., 2010. Immunology of paracoccidioidomycosis. Anais Brasileiros de Dermatologia 86, 516–524.
Foster, L.-A.A., 2002. Utilization and cell-surface binding of hemin by *Histoplasma capsulatum*. Can. J. Microbiol. 48, 437–442. https://doi.org/10.1139/w02-037.
Frausto da Silva, J.J.R., Williams, R.J.P., 2001. The Biological Chemistry of the Elements: The Inorganic Chemistry of Life, 2nd ed. OUP Oxford.
Ganz, T., 2009. Iron in Innate Immunity: Starve the Invaders. Curr. Opin. Immunol. 21, 63–67. https://doi.org/10.1016/j.coi.2009.01.011.
Grahl, N., Cramer, R.A., 2010. Regulation of hypoxia adaptation: an overlooked virulence attribute of pathogenic fungi? Med. Mycol. 48, 1–15. https://doi.org/10.3109/13693780902947342.
Grahl, N., Puttikamonkul, S., Macdonald, J.M., Gamcsik, M.P., Ngo, L.Y., Hohl, T.M., Cramer, R.A., 2011. *In vivo* hypoxia and a fungal alcohol dehydrogenase influence the pathogenesis of invasive pulmonary aspergillosis. PLoS Pathog. 7. https://doi.org/10.1371/journal.ppat.1002145.
Grahl, N., Shepardson, K.M., Chung, D., Cramer, R.A., 2012. Hypoxia and Fungal Pathogenesis: To Air or Not To Air? Eukaryot Cell 11, 560–570. https://doi.org/10.1128/EC.00031-12.
Grossklaus, D.A., Bailão, A.M., Vieira Rezende, T.C., Borges, C.L., de Oliveira, M.A.P., Parente, J.A., de Almeida Soares, C.M., de Arruda Grossklaus, D., Bailão, A.M., Vieira Rezende, T.C., Borges, C.L., de Oliveira, M.A.P., Parente, J.A., de Almeida Soares, C.M., 2013. Response to oxidative stress in *Paracoccidioides* yeast cells as determined by proteomic analysis. Microbes Infect. 15, 347–364. https://doi.org/10.1016/j.micinf.2012.12.002.
Hanslin, H.M., Sæbø, A., Bergersen, O., 2005. Estimation of oxygen concentration in the soil gas phase beneath compost mulch by means of a simple method. Urban For. Urban Greening 4, 37–40. https://doi.org/10.1016/j.ufug.2005.05.001.
Hillmann, F., Linde, J., Beckmann, N., Cyrulies, M., Strassburger, M., Heinekamp, T., Haas, H., Guthke, R., Kniemeyer, O., Brakhage, A.A., 2014. The novel globin protein fungoglobin is involved in low oxygen adaptation of *Aspergillus fumigatus*. Mol. Microbiol. 93, 539–553. https://doi.org/10.1111/mmi.12679.
Hoogewijs, D., Dewilde, S., Vierstraete, A., Moens, L., Vinogradov, S.N., 2012. A phylogenetic analysis of the globins in Fungi. PLoS ONE 7, 1–15. https://doi.org/10.1371/journal.pone.0031856.
Hoot, S.J., Oliver, B.G., White, T.C., 2008. *Candida albicans* UPC2 is transcriptionally induced in response to antifungal drugs and anaerobicity through Upc2p-dependent and -independent mechanisms. Microbiology 154, 2748–2756. https://doi.org/10.1099/mic.0.2008/017475-0.
Horton, P., Park, K.J., Obayashi, T., Fujita, N., Harada, H., Adams-Collier, C.J., Nakai, K., 2007. WoLF PSORT: Protein localization predictor. Nucleic Acids Res. 35. https://doi.org/10.1093/nar/gkm259.
Hutter, J., 2012. Car-Parrinello molecular dynamics. Wiley Interdisciplinary Rev.: Computational Mol. Sci. 2, 604–612. https://doi.org/10.1002/wcms.90.
Jaskiewicz, N.M., Townson, D.H., 2019. Hyper-O-GlcNAcylation promotes epithelial-mesenchymal transition in endometrial cancer cells. Oncotarget 10, 2899–2910. https://doi.org/10.18632/oncotarget.26884.
Kaim, W., Schwederski, B., Klein, A., 2013. Bioinorganic Chemistry - Inorganic elements in the Chemistry of Life: An Introduction and Guide, 2nd ed. Wiley.
Larkin, M.A., Blackshields, G., Brown, N.P., Chenna, R., McGettigan, P.A., McWilliam, H., Valentin, F., Wallace, I.M., Wilm, A., Lopez, R., Thompson, J.D., Gibson, T.J., Higgins, D.G., 2007. Clustal W and Clustal X version 2.0. Bioinformatics 23, 2947–2948. https://doi.org/10.1093/bioinformatics/btm404.
Li, T., Bonkovsky, H.L., Guo, J., 2011. Structural analysis of heme proteins: implications for design and prediction. BMC Struct. Biol. 11, 13. https://doi.org/10.1186/1472-6807-11-13.
Lima, P.S., Casaletti, L., Bailão, A.M., de Vasconcelos, A.T.R., da Fernandes, G.R., de Soares, C.M.A., 2014. Transcriptional and Proteomic Responses to Carbon Starvation in *Paracoccidioides*. PLoS Negl.Trop. Dis. 8. https://doi.org/10.1371/journal.pntd.0002855.
Lima, P.S., Chung, D., Bailão, A.M., Cramer, R.A., de Soares, C.M.A., 2015. Characterization of the *Paracoccidioides* Hypoxia Response Reveals New Insights into Pathogenesis Mechanisms of This Important Human Pathogenic Fungus. PLoS Negl.Trop. Dis. 9, 1–25. https://doi.org/10.1371/journal.pntd.0004282.
Martinez, R., 2017. New Trends in Paracoccidioidomycosis Epidemiology. J. Fungi (Basel) 3. https://doi.org/10.3390/jof3010001.
Nardini, M., Pesce, A., Thijs, L., Saito, J.a., Dewilde, S., Alam, M., Ascenzi, P., Coletta, M., Ciaccio, C., Moens, L., Bolognesi, M., 2008. Archaeal protoglobin structure indicates new ligand diffusion paths and modulation of haem-reactivity. EMBO Rep. 9, 157–163. https://doi.org/10.1038/sj.embor.7401153.
Page, R.D., 1996. TreeView: an application to display phylogenetic trees on personal computers. Comput. App. Biosci.: CABIOS 12, 357–358.
Parente, A.F.A., Bailão, A.M., Borges, C.L., Parente, J.A., Magalhães, A.D., Ricart, C.A.O., Soares, C.M.A., 2011. Proteomic analysis reveals that iron availability alters the metabolic status of the pathogenic fungus *Paracoccidioides brasiliensis*. PLoS ONE 6. https://doi.org/10.1371/journal.pone.0022810.
Parente, A.F.A., de Rezende, T.C.V., de Castro, K.P., Bailão, A.M., Parente, J.A., Borges, C.L., Silva, L.P., de Soares, C.M.A., 2013. A proteomic view of the response of *Paracoccidioides* yeast cells to zinc deprivation. Fungal Biology 117, 399–410. https://doi.org/10.1016/j.funbio.2013.04.004.
Parente, A.F.A., Naves, P.E.C., Pigosso, L.L., Casaletti, L., McEwen, J.G., Parente-Rocha, J.A., Soares, C.M.A., 2015. The response of *Paracoccidioides* spp. to nitrosative stress. Microbes Infect. 17, 575–585. https://doi.org/10.1016/j.micinf.2015.03.012.
Parente-Rocha, J.A., Parente, A.F.A., Baeza, L.C., Bonfim, S.M.R.C., Hernandez, O., McEwen, J.G., Bailão, A.M., Taborda, C.P., Borges, C.L., de Soares, C.M.A., 2015. Macrophage Interaction with *Paracoccidioides brasiliensis* Yeast Cells Modulates Fungal Metabolism and Generates a Response to Oxidative Stress. PLoS ONE 10, e0137619. https://doi.org/10.1371/journal.pone.0137619.
Pigosso, L.L., Baeza, L.C., Tomazett, M.V., Faleiro, M.B.R., de Moura, V.M.B.D., Bailão, A.M., Borges, C.L., Rocha, J.A.P., Fernandes, G.R., Gauthier, G.M., de Soares, C.M.A., 2017. *Paracoccidioides brasiliensis* presents metabolic reprogramming and secretes a serine proteinase during murine infection. Virulence 1–18. https://doi.org/10.1080/21505594.2017.1355660.
Portis, I.G., de Sousa Lima, P., Paes, R.A., Oliveira, L.N., Pereira, C.A., Parente-Rocha, J.A., Pereira, M., Nosanchuk, J.D., de Almeida Soares, C.M., 2020. Copper overload in *Paracoccidioides lutzii* results in the accumulation of ergosterol and melanin. Microbiol. Res. 239, 126524. https://doi.org/10.1016/j.micres.2020.126524.
Poulos, T.L., 2014. Heme Enzyme Structure and Function. Chem. Rev. https://doi.org/10.1021/cr400415k.
Prado, M., da Silva, M.B., Laurenti, R., Travassos, L.R., Taborda, C.P., 2009. Mortality due to systemic mycoses as a primary cause of death or in association with AIDS in Brazil: A review from 1996 to 2006. Mem. Inst. Oswaldo Cruz 104, 513–521. https://doi.org/10.1590/S0074-02762009000300019.
Pronk, S., Páll, S., Schulz, R., Larsson, P., Bjelkmar, P., Apostolov, R., Shirts, M.R., Smith, J.C., Kasson, P.M., Van Der Spoel, D., Hess, B., Lindahl, E., 2013. GROMACS 4.5: A high-throughput and highly parallel open source molecular simulation toolkit. Bioinformatics 29, 845–854. https://doi.org/10.1093/bioinformatics/btt055.
Rappleye, C.A., Engle, J.T., Goldman, W.E., 2004. RNA interference in Histoplasma capsulatum demonstrates a role for α-(1,3)-glucan in virulence. Mol. Microbiol. 53, 153–165. https://doi.org/10.1111/j.1365-2958.2004.04131.x.
Restrepo, A., McEwen, J.G., Castañeda, E., 2001. The habitat of *Paracoccidioides brasiliensis*: how far from solving the riddle? Med. Mycol. 39, 233–241.
Rezende, T.C.V., Borges, C.L., Magalhães, A.D., de Sousa, M.V., Ricart, C.A.O., Bailão, A.M., Soares, C.M.A., 2011. A quantitative view of the morphological phases of *Paracoccidioides brasiliensis* using proteomics. J. Proteomics 75, 572–587. https://doi.org/10.1016/j.jprot.2011.08.020.
Rocha, S., 2007. Gene regulation under low oxygen: holding your breath for transcription. Trends Biochem. Sci. 32, 389–397. https://doi.org/10.1016/j.tibs.2007.06.005.
Rodrigues, L.N.S., de Brito, W.A., Parente, A.F.A., Weber, S.S., Bailão, A.M., Casaletti, L., Borges, C.L., de Soares, C.M.A., 2016. Osmotic stress adaptation of *Paracoccidioides lutzii*, *Pb*01, monitored by proteomics. Fungal Genet. Biol. 95, 13–23. https://doi.org/

10.1016/j.fgb.2016.08.001.
Saitou, N., Nei, M., 1987. The neighbor-joining method: a new method for reconstructing phylogenetic trees. Mol. Biol. Evol. 4, 406–425.
Sambrook, J., Russel, D.W., 2001. Molecular Cloning. A Laboratory Manual. Cold Spring Harbor Laboratory Press, New York.
Silva, M.G., de Curcio, J.S., Silva-Bailão, M.G., Lima, R.M., Tomazett, M.V., de Souza, A.F., Cruz-Leite, V.R.M., Sbaraini, N., Bailão, A.M., Rodrigues, F., Pereira, M., Gonçales, R.A., de Almeida Soares, C.M., 2020. Molecular characterization of siderophore biosynthesis in *Paracoccidioides brasiliensis*. IMA Fungus 11, 11. https://doi.org/10.1186/s43008-020-00035-x.
Silva-Bailão, M.G., Bailão, E.F.L.C., Lechner, B.E., Gauthier, G.M., Lindner, H., Bailão, A.M., Haas, H., Soares, C.M.D.A., 2014. Hydroxamate production as a high affinity iron acquisition mechanism in *Paracoccidioides* Spp. PLoS ONE 9. https://doi.org/10.1371/journal.pone.0105805.
Simmen, H.P., Battaglia, H., Giovanoli, P., Blaser, J., 1994. Analysis of pH, pO2 and pCO2 in drainage fluid allows for rapid detection of infectious complications during the follow-up period after abdominal surgery. Infection 22, 386–389.
Steentoft, C., Vakhrushev, S.Y., Joshi, H.J., Kong, Y., Vester-Christensen, M.B., Schjoldager, K.T.-B.G.B.G., Lavrsen, K., Dabelsteen, S., Pedersen, N.B., Marcos-Silva, L., Gupta, R., Paul Bennett, E., Mandel, U., Brunak, S., Wandall, H.H., Levery, S.B., Clausen, H., 2013. Precision mapping of the human O-GalNAc glycoproteome through SimpleCell technology. EMBO J. 32, 1478–1488. https://doi.org/10.1038/emboj.2013.79.
Stranava, M., Man, X.P., Skálova, X.T., Kolenko, X.P., Blaha, X.J., Fojtikova, X.V., Martínek, X.V., Dohnálek, X.J., Lengalova, A., Rosulek, X.M., Shimizu, T., Martínková, X.M., 2017. Coordination and redox state-dependent structural changes of the heme-based oxygen sensor AfGcHK associated with intraprotein signal transduction. J. Biol. Chem. 292, 20921–20935. https://doi.org/10.1074/jbc.M117.817023.
Synnott, J.M., Guida, A., Mulhern-Haughey, S., Higgins, D.G., Butler, G., 2010. Regulation of the Hypoxic Response in *Candida albicans*. Eukaryot. Cell 9, 1734–1746. https://doi.org/10.1128/EC.00159-10.
Thompson, J.D., Gibson, T.J., Plewniak, F., Jeanmougin, F., Higgins, D.G., 1997. The CLUSTAL X windows interface: Flexible strategies for multiple sequence alignment aided by quality analysis tools. Nucleic Acids Res. 25, 4876–4882. https://doi.org/10.1093/nar/25.24.4876.
Todd, B.L., Stewart, E.V., Burg, J.S., Hughes, A.L., Espenshade, P.J., 2006. Sterol Regulatory Element Binding Protein Is a Principal Regulator of Anaerobic Gene Expression in Fission Yeast. Mol. Cell. Biol. 26, 2817–2831. https://doi.org/10.1128/MCB.26.7.2817-2831.2006.
Torres, I., Hernandez, O., Tamayo, D., Muñoz, J.F., García, A.M., Gómez, B.L., Restrepo, A., McEwen, J.G., 2014. *Paracoccidioides brasiliensis Pb*P27 gene: knockdown procedures and functional characterization. FEMS Yeast Res. 14, 270–280. https://doi.org/10.1111/1567-1364.12099.
Vik, A., Rine, J., 2001. Upc2p and Ecm22p, dual regulators of sterol biosynthesis in *Saccharomyces cerevisiae*. Mol. Cell. Biol. 21, 6395–6405. https://doi.org/10.1128/mcb.21.19.6395-6405.2001.
Vinogradov, S.N., Hoogewijs, D., Bailly, X., Mizuguchi, K., Dewilde, S., Moens, L., Vanfleteren, J.R., 2007. A model of globin evolution. Gene 398, 132–142. https://doi.org/10.1016/j.gene.2007.02.041.
Willger, S.D., Puttikamonkul, S., Kim, K.-H., Burritt, J.B., Grahl, N., Metzler, L.J., Barbuch, R., Bard, M., Lawrence, C.B., Cramer, R.A., 2008. A sterol-regulatory element binding protein is required for cell polarity, hypoxia adaptation, azole drug resistance, and virulence in *Aspergillus fumigatus*. PLoS Pathog. 4, e1000200. https://doi.org/10.1371/journal.ppat.1000200.
Yang, J., Roy, A., Zhang, Y., 2013. Protein-ligand binding site recognition using complementary binding-specific substructure comparison and sequence profile alignment. Bioinformatics 29, 2588–2595. https://doi.org/10.1093/bioinformatics/btt447.
Yang, J., Yan, R., Roy, A., Xu, D., Poisson, J., Zhang, Y., 2014. The I-TASSER suite: Protein structure and function prediction. Nat. Methods 12, 7–8. https://doi.org/10.1038/nmeth.3213.
Yang, J., Zhang, Y., 2016. Protein structure and function prediction using I-TASSER. Current Protocols in Bioinformatics 1–24. https://doi.org/10.1002/0471250953.bi0508s52.Protein.
Zhang, C., Freddolino, P.L., Zhang, Y., 2017. COFACTOR: Improved protein function prediction by combining structure, sequence and protein-protein interaction information. Nucleic Acids Res. 45, W291–W299. https://doi.org/10.1093/nar/gkx366.
Zhang, V., Nemeth, E., Kim, A., 2019. Iron in Lung Pathology. Pharmaceuticals (Basel) 12. https://doi.org/10.3390/ph12010030.
Zhang, W., Phillips, G.N., 2003. Structure of the oxygen sensor in *Bacillus subtilis*: Signal transduction of chemotaxis by control of symmetry. Structure 11, 1097–1110. https://doi.org/10.1016/S0969-2126(03)00169-2.